IEEE Access
Multidisciplinary | Rapid Review | Open Access Journal

Received August 24, 2021, accepted September 2, 2021, date of publication September 7, 2021,
date of current version September 15, 2021.

Digital Object Identifier 10.1109/ACCESS.2021.3110816

Evaluating Drought Events by Time-Frequency Analysis: A Case Study in Aegean Region of Turkey

SEMRA KOCAASLAN[1], NEBİYE MUSAOĞLU[2], AND SAEID KARAMZADEH[3]
[1]Department of Applied Informatics, Geographical Information Technologies Program, Istanbul Technical University, 34469 Istanbul, Turkey
[2]Department of Geomatics Engineering, Istanbul Technical University, 34469 Istanbul, Turkey
[3]Electrical and Electronics Engineering Department, Faculty of Engineering and Natural Sciences, Bahçeşehir University, 34353 Istanbul, Turkey

Corresponding author: Semra Kocaaslan (kocaaslan@itu.edu.tr)

ABSTRACT Drought is a slowly progressing and complex natural phenomenon, so the nature of drought events remains unclear. Remote sensing is preferred as an effective tool for finding, evaluating, and monitoring drought especially for large areas throughout long-term periods by providing near real-time and accurate data. Besides, Google Earth Engine (GEE) is a cloud-based service to provide analysis and visualization of geospatial datasets. The ability of GEE as a remote sensing platform to analyze high-impact societal issues, including water management diseases, disaster, deforestation, and climate monitoring environmental protection, offers it as the best option for drought monitoring. Here, Vegetation Health Index (VHI) index that combines Vegetation Condition Index (VCI) and Temperature Condition Index (TCI) has been chosen for agricultural drought assessment in a case study (Aegean Region of Turkey) from 2000 to 2018 (19 years). Thence, the land surface temperature (LST) data and the Normalized Difference Vegetation Index (NDVI) data from the Moderate Resolution Imaging Spectroradiometer (MODIS) sensor have been used and analyzed as remotely sensed data. The major data processing steps have been efficiently done on the GEE platform. Also, the time series and periodic behavior of these satellite-based indices have been examined. Besides, as the meteorological drought index, Standardized Precipitation Evapotranspiration Index (SPEI) time series were calculated for the region in question at different time scales (SPEI3, SPEI6, SPEI12, etc.) from 1980 to 2018 (39 years). Also, the frequency analysis of both satellite-based and meteorological station-based indices has been done. Fast Fourier Transform (FFT) for satellite-based indices frequency analyzing and Wavelet Transform (WT) for time-frequency analyzing of SPEI sequence have been used. Cross Wavelet (XWT), and Coherence Wavelet (CWT) were used to evaluate the time-frequency relationship of the satellite-based and the meteorological station-based time series.

INDEX TERMS Drought, drought monitoring, VCI, TCI, VHI, SPEI.

I. INTRODUCTION

Drought is different in that its characteristics are unique compared to other natural disasters. Because of its nature, it is difficult to detect and monitor the onset, severity, and duration [1], [2]. Also, the effects of droughts may come on gradually over time and may have different effects by spreading over large areas [3]. It can occur anywhere and anytime and has devastating effects on environmental, social, and economic sectors [4], [5].

The associate editor coordinating the review of this manuscript and approving it for publication was Stefania Bonafoni.

According to the different sectors affected, drought events are divided into four main categories. The meteorological drought is descriptive of the amount of rainfall over a long period to remain below the average amount of precipitation belonging to that region. Agricultural drought could be defined as the period when the value of soil moisture is lower than that required for plant growth and development. Hydrological drought, indicates that the amount of water in surface and groundwater resources decreases as a result of long-term insufficient rainfall, and socioeconomic drought describes the effects of drought on water resources, agriculture, life, and industries that benefit from it [1], [6], [7].

During the last decades, numerous methods have been adopted to monitor and numerically describe drought through the development of drought indices applied in the areas of meteorology, hydrology, and agriculture, [8]–[11]. Traditional approaches of drought monitoring generally rely on indices derived from meteorological station parameters like precipitation. The Standardized Precipitation Index (SPI) [12] recommended by the World Meteorological Organization (WMO), is one of the most widely used meteorological drought indexes solely based on this parameter [3]. However, other meteorological parameters (e.g. evapotranspiration and temperature) also affect drought occurrence and severity. The Standardized Precipitation Evapotranspiration Index (SPEI) [13] proposed by Vicente-Serrano *et al.* is an index based not only on precipitation but also on potential evapotranspiration (PET). Similar to the SPI, SPEI can be calculated for time scales ranging from 1 to 48 months [14].However, Ji and Peters [15] suggested that a 3-month SPI and, also SPEI is better to monitor drought impact on vegetation.

While station-based traditional approaches require continuous historical data for drought monitoring, satellite-based methods give fast and reasonable results for near real-time acquisition, drought analysis, with wide and continuous spatial coverage. As a satellite-based index, the Normalized Vegetation Index (NDVI) was first applied to drought monitoring by Tucker and Choudhury [16]. The most widely used satellite-based vegetation index, NDVI, is an operational indicator of vegetation moisture status [15], [17]–[20]. In addition to NDVI, Land Surface Temperature (LST or Ts) parameters obtained from thermal bands of satellites were used to promote drought indices [19]–[22]. Then, different vegetation indices (VIs) were developed, such as the Vegetation Condition Index (VCI) derived from NDVI, which provides an improvement for analysis of vegetation conditions without weathering, especially in non-homogeneous areas [23], [24]. Because of more sensitivity to water stress [11], the temperature was also utilized to develop drought indices as the Temperature Condition Index (TCI) [25]. Since the combination of NDVI and LST provides information on both vegetation and moisture status, drought indices like VCI and TCI can effectively evaluate drought conditions. Last but not least, the Vegetation Health Index (VHI) which relies on an empirical combination of VCI and TCI was developed by Kogan [26], [27].

The Google Earth Engine (GEE) is a fast, online, and cloud-based data-monitoring platform for calculating and illustrating the satellite-based raw and processed data. The GEE can use Google's massive computing capabilities that combine data from the National Aeronautics and Space Administration (NASA) [28], [29]. Therewithal, GEE's advantages are to examine large-scale remote sensing datasets, review time series, and download results instantly using Google's high-performance parallel computing service. In particular, the GEE has been very useful in drought analysis and monitoring.

Moreover, investigating the time series seasonal pattern and frequency behavior of the drought is crucial for many phenomena as drought monitoring, drought forecasting, and spatio-temporal characteristics analysis [30], [31].

One of the most powerful methods used to perform frequency analysis is the Fourier transform (FT). The FT divides time-domain data into different components and specifies the repetition period and frequency of each. In this way, it can be seen how and how often each event occurred in the past, and forward-looking implications can be found.

For non-stationary signals (time series), frequency analysis should be done on the time scale. In this instance, time-frequency transform methods, like Short-Time Fourier Transform (STFT) and Wavelet Transform (WT) are beneficial [32]–[35]. For validation and making a more reliable gang up, it makes sense to explore the correlation between meteorological drought and satellite-based drought indices. For this purpose, cross wavelet and coherence wavelet are introduced.

This study aims to monitor and analyze the frequency and severity of drought to characterize the probability of occurrence of droughts of various magnitudes. For this purpose, SPEI and VHI (also VCI and TCI two-components of it) indices were adopted. Spectral characteristics of drought are investigated based on the Fast Fourier Transform (FFT), Short-Time Fourier Transform (STFT), and Wavelet Transform (WT) methods. For the first time, the time-frequency correlation between satellite-based drought indices and meteorological station-based drought indices (SPEI) has been analyzed. The satellite-based drought index results made in GEE, the meteorological station-based result (SPEI), the frequency analysis, and time-frequency correlations made in the MATLAB program for the mentioned region and dates are presented in the next sections.

II. CASE STUDY AND DATA

A. CASE STUDY

The Aegean Region is one of the seven geographical regions of Turkey divided according to different climatic conditions and topography. The region (38° 57' 58'' North 28° 43' 14'' East), is located in the western part of the country that garners its name from the Aegean Sea (Figure 1). Since in the Aegean coast, where the mountain ranges trend perpendicular to the shoreline, wide plains extend between the ranges to the plateaus of the interior, sea climate can also enter inland areas [36]. On the other hand, the climate around the coastline is partially different from the inner region climate due to the increase in altitude towards the inner parts and departure from the sea effect [37].

The region which is under the impact of the Mediterranean climatic regime has cool, rainy winters, and mostly hot, dry summers at the coast and a semi-arid continental climate in the interior with hot, dry summers and cold, snowy winters [38]. In this region, precipitation is usually more in January. The climate becomes intermittent due to the increase

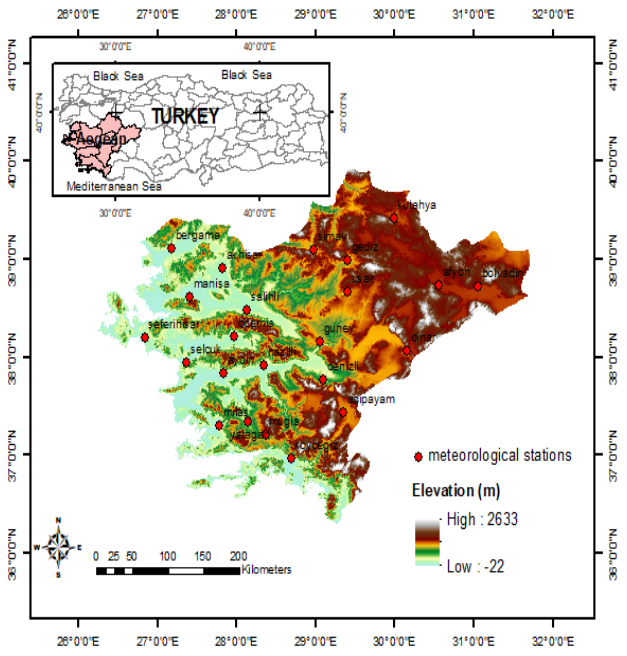

FIGURE 1. The location and topography of the Aegean Region and spatial distributions of meteorological stations.

in altitude and the distance to the sea as one goes to the Inner West Anatolia section. Besides, the contribution of the region to the domestic economy is mostly in the field of agriculture. Depending on the differences in climate and landforms among the departments, there are also differences and varieties among the products grown. Tobacco, cotton, olives, figs, citrus fruits, grapes, poppy, and cereals are the main crops grown in the region.

Furthermore, according to the Fifth Assessment Report (AR5) of the Intergovernmental Panel on Climate Change (IPCC), there is substantial evidence that anthropogenic global warming has led to an increase in drought frequency, intensity, and/or the amount of drought in the region, including the Mediterranean region [39]. Hence, the drought-prone Aegean Region, which is a part of the greater Mediterranean Basin, was chosen as the case study.

B. REMOTELY SENSED DATA

MODerate Resolution Imaging Spectroradiometer (MODIS) with the Terra and Aqua satellites could view the entire Earth's surface every 1 to 2 days and gather data in 36 spectral bands (optical and thermal) ranging in wavelength from 0.4 μm to 14.4 μm at resolutions of 250 m to 1 km. For this study, MOD11A2.006 Terra Land Surface Temperature (LST) 8-day with 1km *(https://doi.org/10.5067/MODIS/MOD11A2.006)* and MOD13A2.006 Terra Vegetation Indices (NDVI) *(https://doi.org/10.5067/MODIS/MOD13A2.006)* 16-day with 1 km products were compiled as remote sensing data sources on the GEE platform. All the satellite-based data set have been averaged to monthly scales the period to be compatible with the monthly in situ data. To calculate the time series of vegetation indices (VIs)-based and temperature-based drought indices, the monthly data of 2000–2018 period were utilized.

C. IN-SITU DATA

In this study; geographical coordinates, monthly mean temperature (°C), and monthly total precipitation (mm = kg/m^2) data of 23 gauging stations covering the years 1980-2018 used as in-situ data were obtained from the Turkish State Meteorological Service) (https://mevbis.mgm.gov.tr/mevbis/ui/index.html/Login). Because of the discontinuities in the data from some gauging stations and the lack of data in some years, we chose the stations that best represent the Aegean Region from the homogeneously distributed stations for meteorological data.The locations of the stations are shown in Figure 1.

III. METHODOLOGY

A. DROUGHT INDICES

1) VEGETATION CONDITION INDEX

The Vegetation Condition Index (VCI) is considered an improvement in the analysis of vegetation conditions, especially for non-homogeneous areas [23], [27]. VCI can extract the weather impact on vegetation while removing the ecosystem signal from the NDVI [24], and is defined as the following;

$$VCI_{ij}^{k} = 100 * \frac{NDVI_{ij}^{k} - min(NDVI_{i}^{k})}{max(NDVI_{i}^{k}) - min(NDVI_{i}^{k})} \quad (1)$$

where $NDVI_{ij}^{k}$ indicates the values for pixel i in month j for year k, extracted from the long-term record and $max(NDVI_{i}^{k})$ and $min(NDVI_{i}^{k})$ maximum and minimum NDVI values in the period, respectively. VCI varies from 0 to 100; VCI below 40 indicates stressed vegetation conditions [26], [40], [41]. Therefore, indices below 40 are accepted as the beginning of a drought.

2) TEMPERATURE CONDITION INDEX

Temperature Condition Index (TCI) uses land surface temperature (LST) derived from the thermal infrared bands of MODIS. TCI is related to the altered response of vegetation to temperature. The following equation shows its formula:

$$TCI_{ij}^{k} = 100 * \frac{max(LST_{i}^{k}) - LST_{ij}^{k}}{max(LST_{i}^{k}) - min(LST_{i}^{k})} \quad (2)$$

where LST_{ij}^{k} means for each pixel (k), month (i), and year (j) value extracted from multiyear time series data and $max(LST_{i}^{k})$ and $min(LST_{i}^{k})$ are the maximum and minimum values of LST, respectively for the same point over the research period 2000 - 2018. Unlike the NDVI, higher surface temperature reflect drought conditions and lower values show favorable conditions [25]. Thus, TCI_{ij}^{k} values vary from 0 to 100, indicating stress to good thermal conditions of the vegetation.

TABLE 1. Drought classification scheme of VHI [26].

VHI range	Drought Class
0 to 10	Extreme Drought
10 to 20	Severe Drought
20 to 30	Moderate Drought
30 to 40	Mild Drought
more than 40	No Drought

3) VEGETATION HEALTH INDEX

This index is based on the VCI and TCI combinations, which is a useful source of information regarding the stress on vegetation by drought and is calculated using the following equation:

$$VHI_{ij}^{k} = \alpha VCI_{ij}^{k} - (1-\alpha)TCI_{ij}^{k} \tag{3}$$

where α is a weight parameter associated with VCI and TCI. Kogan [25], decided to load a higher weight for VCI using a value of 0.7 for VCI and 0.3 for TCI, and also there are different studies with different weights [26], [27], [42]. Since there was no a priori knowledge about the contribution of VCI and TCI to vegetation health, weights were taken equally (0.5) in this study. The VCI, TCI, and VHI values vary from 0 (severe vegetation stress) to 100 (optimal vegetation conditions) [43]. Table 1 indicates the drought classification according to the VHI threshold values.

4) STANDARDIZED PRECIPITATION EVAPOTRANSPIRATION INDEX

The SPEI which is based on precipitation (P) and potential evapotranspiration (PET) data represents a basic climatological water balance calculated at different time scales [13]. PET can be calculated using the Thornthwaite, Penman-Monteith, or Hargreaves methods. The monthly PET (mm) is obtained by

$$PET = 16K\left(\frac{10T}{I}\right)^{m} \tag{4}$$

where; T is the monthly-mean temperature (°C); I is the heat index and m is a coefficient dedicated as a third-order polynomial dependent on heat index. The K is a correction coefficient depending on the latitude of the region and month and acquired by

$$K = \left(\frac{N}{12}\right)\left(\frac{NDM}{30}\right) \tag{5}$$

where; NDM is the number of days of the month and N is the maximum number of sun hours. The difference (D) is calculated by the difference between precipitation P and PET for month j,

$$Dj = Pj - PETj \tag{6}$$

The traditional approximation of Abramowitz and Stegun [44] to obtain the SPEI is as follows:

$$SPEI = W - \frac{C_0 + C_1 W + C_2 W^2}{1 + d_1 W + d_2 W^2 + d_3 W^3} \tag{7}$$

$$W = \sqrt{-2ln(Pr)} \quad pr \le 0.5 \tag{8}$$

$$Pr = 1 - F(x) \tag{9}$$

TABLE 2. Drought classification scheme according to SPEI [13].

SPEI value	Category
+2.0 and more	Extremely Wet
1.5 to 1.99	Very Wet
1.0 to 1.49	Moderately Wet
-.99 to .99	Near Normal
-1.0 to -1.49	Moderately Drought
-1.5 to -1.99	Severely Drought
-2 and less	Extremely Drought

Pr is the exceedance of probability of a determined D value. When Pr $>$ 0.5, then Pr is replaced by $1 - Pr$, and the sign of the resultant SPEI is reversed. The constants are $C_0 = 2.515517$, $C_1 = 0.8022853$, $C_2 = 0.010328$, $d_1 = 1.432788$, $d_2 = 0.189269$ and $d_3 = 0.001308$. The difference between precipitation (P) and potential evapotranspiration (PET) is used to calculate the SPEI [13].

In our case, the Thornthwaite approach [45] was adopted to calculate PET because of its simplicity and efficiency in calculating using only monthly mean temperature and precipitation data. SPEI was calculated for the region in question at different time scales (SPEI 3, SPEI 6, SPEI 12, etc.) for the related period by R software SPEI package. Since the interest of this study is to focus both meteorological and agricultural drought, we mainly focused on SPEI-3 as it provides better results for monitoring the impact of drought on vegetation [7], [15]. Also, drought classification according to SPEI values was completed as shown in Table 2.

B. FREQUENCY ANALYSIS METHODS

1) FAST FOURIER TRANSFORM (FFT)

The FT is used to describe signals in the time or spatial domains. The FT could decompose a function into a sum of different sinusoidal functions with different amplitudes, phases, and frequencies [46], [47].

Besides, for analyzing the sampled data and discrete data the discrete Fourier transform (DFT) is used as a counterpart to FT [48]. The DFT is implemented in sampled, discrete, and digital data by a family of algorithms in the lump known as the FFT. In comparison with the DFT, the FFT reduces the computing workload significantly. The N2 complex operations (adds and multiplies) are needed in the DFT, meanwhile, the FFT could be carried out just with workloads between 2 $\times$ N and log2(N) $\times$ N/2 complex operations [49]. The time series consists of several signals that have different amplitudes and periods. The FFT transfers the time series from the time domain to the frequency domain and indicates the frequency properties of each signal. This ability can be used advantageously for time series harmonics analyzing and forecasting [50]–[52].

C. SHORT-TIME FOURIER TRANSFORM (STFT)

One of the effective tools for analyzing non-stationary signals is STFT. The STFT is able to divide the times series into equal parts, called time windows, and analyze the spectrum of each window [53], [54].

The STFT equation to $x(t)$ signal is shown below, where τ is the spectrum localization time and $g(t)$ is the window function.

$$STFT(\tau, f) = \int_{-\infty}^{\infty} x(t)g(\tau - t)e^{-j2\pi ft}\, dt \tag{10}$$

D. WAVELET TRANSFORM (WT)

The WT is another efficient method for analyzing a non-stationary time series containing different frequencies in different time scales. The WT also provides a two-dimensional localized time-frequency analysis [55], [56]. Compared to STFT, which is a permanent window function, the window function of the WT is scalable and shiftable over time. This property will increase the analysis resolution. Hence, WT has been used for investigating the temporal variability of rainfall, runoff, and climate variability as an effective tool for analyzing the statistical properties of the time series [57]–[60]. Mathematically Continues Wavelet Transform (CWT) could be expressed as follows [61];

$$C(a, b) = \frac{1}{\sqrt{a}} \int s(t)\psi(\frac{t-b}{a})\, dt \tag{11}$$

where a is scale function, b is the position function, $s(t)$ is the signal (time series), and ψ is the mother wavelet function. The representation of the CWT value as a function of time and frequency is a scalogram. Instantaneous frequencies during the duration of the signal can be accurately estimated with CWT [62]. The wavelet power spectrum can be used to state the mutation features and multiscale evolution of time series and sequences. The equation of the wavelet power spectrum can be mentioned as [63]:

$$Wx(a, \tau) = C_x(a, \tau)C_x^*(a, \tau) = |C_x(a, \tau)| \tag{12}$$

where $C_x(a, \tau)$ is the wavelet transform coefficient and $C_x^*(a, \tau)$ is the complex conjugate of the wavelet transform coefficient.

E. CROSS WAVELET AND COHERENCE

The cross wavelet transform (XWT) is an analysis method for the assessment of the correlation between two-time series. Details and the phase structure could be examined in the time domain and frequency domain [61]. If the CWT of the considered Xn and Yn sequences are $W_n^X(s)$ and $W_n^Y(s)$ respectively, the XWT is defined as:

$$W_n^X Y(s) = W_n^X(s)\, W_n^{Y*}(s) \tag{13}$$

Also, the resonance information of the two sequences in the time-frequency domain could be obtained by the XWT spectrum power that is defined by the absolute values of the equation 11. The complex argument $arg(W_n^X Y(s))$ indicates the local phase information between the two $W_n^X(s)$ and $W_n^Y(s)$ sequences in the time-frequency domain. The phase arrows points right if (Xn and Yn) sequences are in-phase, points left if they are anti-phase, points down if Xn leading Yn by 90 degrees and points up if Xn lagging Yn by 90 degrees. Another useful technique is analyzing how coherent the WT is in time-frequency space. The wavelet coherence (WTC) of two-time series is defined as;

$$R_n^2(s) = \frac{|S(s^{-1}W_n^X Y(s))|^2}{S(s^{-1}|(W_n^Y(s)|^2).S(s^{-1}|(W_n^X(s)|^2))} \tag{14}$$

where S is a smoothing operator.

The WTC spectrogram demonstrates the coherence between two WT. The phase spectrum characterizes the response and lag between two-time series, and the phase angle expresses the direction of correlation of two time series in the time-frequency domain.

In a nutshell, the XWT and WTC reflect the consistency and correlation respectively, of the two-time series (satellite-based and ground metrological drought indices time series) in different periods and different time scales.

IV. RESULTS AND DISCUSSION

Monthly VCI has been computed using equation 1 by the GEE platform for the 2000-2018 period for the Aegean Region. Equation 2 has been used for the calculation of TCI for the same period of time. The VCI and TCI results were used for VHI calculation using equation 3.

The results of all indices have been exported and displayed. As an example, the VHI results for the month of July for some years are given in figure 2. It has been clearly established that 2001 and 2007 were drought years.

SPEI was also calculated using the precipitation data obtained from homogeneously distributed meteorological stations. Figure 3 shows the monthly time series of the SPEI results for the Aegean Region from 1980 to 2018. According to this graph, 2007 stands out as the driest year in the calculated years, while 2001, the second driest year, was seen as a drier year compared to 2002, and 2015 was followed as a non-dry year.

In this study, frequency analysis of satellite-based indexes is presented and frequency-based correlation analysis between satellite-based and meteorological-based stations is proposed for the first time in the literature.

To peruse the harmonic attitude of drought time series, FFT has been employed to the VCI, TCI, and VHI indices. Then, periodogram function has been used for better illustration. In periodogram function, the frequency in terms of radians/sample are defined as follows (ω is the normalized frequencies in terms of radians/sample) [48].

$$P(f) = \frac{1}{2\pi N} + |\sum_{n=0}^{N-1} X_n e^{-j\omega n}|^2 \quad -\pi < \omega < \pi \tag{15}$$

The monthly time series of the VCI, TCI, and VHI from 2000 to 2018 years are given in figure 4. Spectral characteristics of drought indices (VCI, TCI, and VHI) are analyzed and the results for the mentioned temporal are shown in figure 5.

The results show that the periodic characteristics of drought patterns for these three indices are so close. The evaluation of the harmonic behavior of drought time series shows that cycles are approximately 5.88, 2.94, and 1.96.

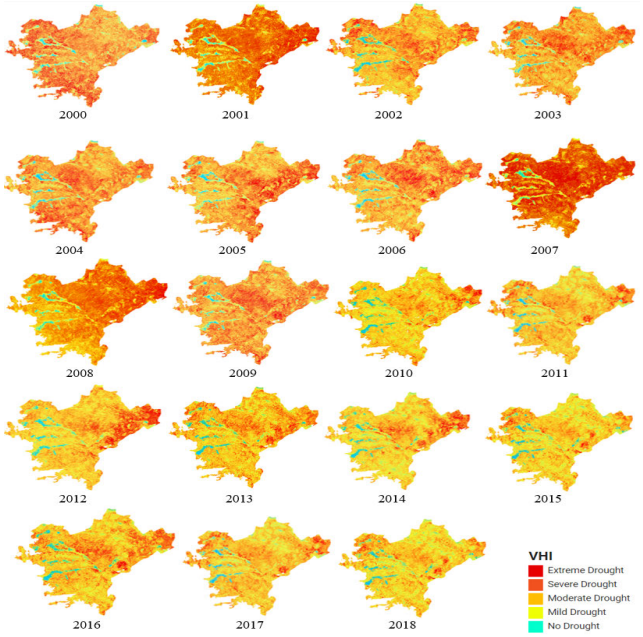

FIGURE 2. Spatio-temporal changes of drought events according to the VHI results.

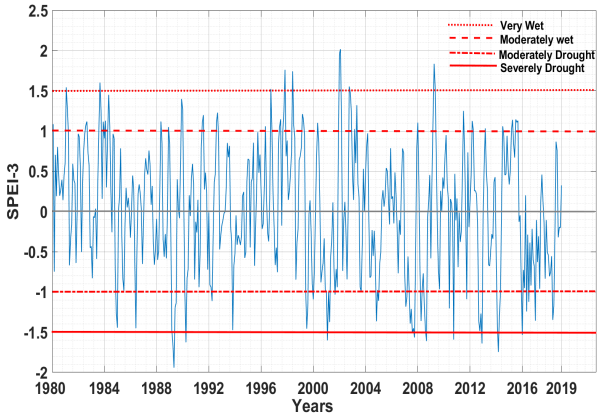

FIGURE 3. Time series of the SPEI-3 results between 1980 and 2018.

The results are in good agreement with the GEE results given before. The drought years and harmonic cycles between these years in spectral analyses have a plausible pattern.

The time series of the satellite-based drought indices (TCI, VCI, and VHI) was stationary data; the harmonic attitudes have been analyzed by FFT in the previous part. Here, Short Time Fourier Transform (STFT) is used for investigating SPEI time series which is a non-stationary signal. STFT based spectrogram is shown in figure 6. SPEI signal in the time domain and amplitude spectrum of the signal (frequency-magnitude and time-frequency) is illustrated. The result shows the frequency and power density spectrum of the time series. The periodic cycle of the SPEI could be deduced considering the dominant frequency.

The wavelet power spectra of the monthly SPEI time series are calculated and shown in figure 7. Concerning the results, some cycles could be mentioned as 10-12 months

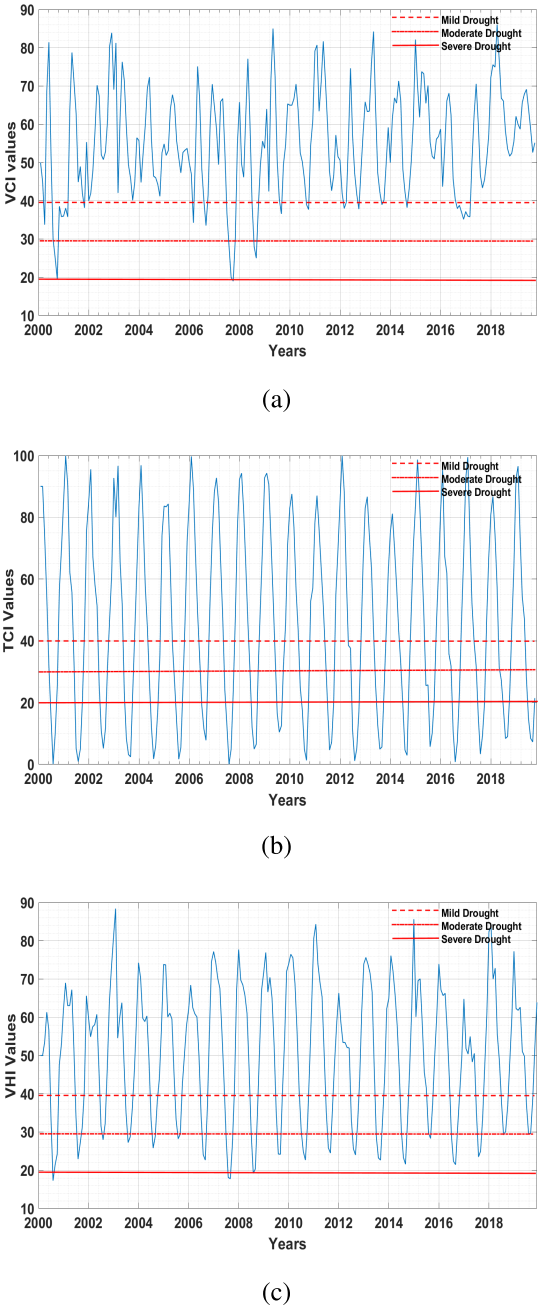

FIGURE 4. Temporal patterns of a) VCI, b) TCI, and c) VHI from 2000 Jan (0) to 2018 Dec (228).

(1988-1992), 12-14 months (2006-2009), and 8-10 months (2012-2015).

Figure 8. depicts the monthly SPEI time series from January 1980 to December 2018 and the real part of CWT. The Morlet is used for computing the wavelet coefficients of the signal at real and positive scales. The magnitude of the wavelet coefficients is represented by the intensity at each x–y point. The large values of the WT coefficients indicate a high correlation between the signal combined with a large fluctuation and the Morlet wavelet featured with a light color

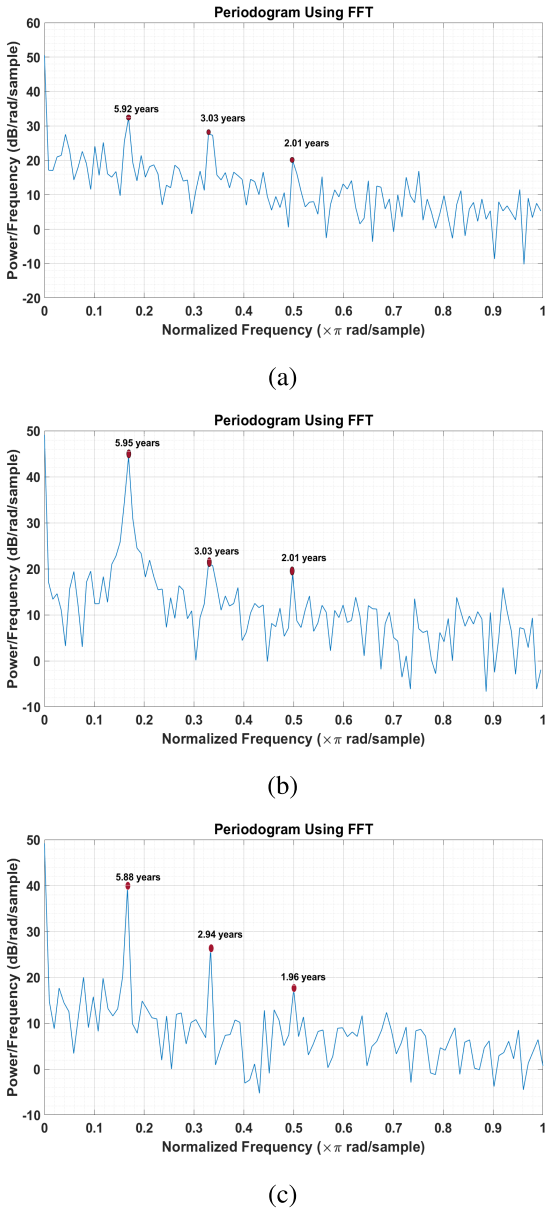

FIGURE 5. Spectral analysis in the selected region based on VCI, TCI, and VHI.

on the figure. Low values of the WT coefficients mean that the Morlet and signal are out of the phase which is shown by a dark color in the wavelet map. The fine granularity in the bottom part of the scale reflects peaks in the SPEI data.

The correlation and coherence between satellite-based drought indices (VCI, TCI, and VHI) and meteorological station-based drought index (SPEI) have been studied from January 2000 to December 2018 (228 months). The XWT and WCT results are shown in figure 9 and figure 10 respectively.

Figure 9 shows the XWT results focused on the relationship between the SPEI time series and the VCI time series, (b) SPEI time series and the TCI time series, and (c) SPEI time series and the VHI time series in the high-energy regions.

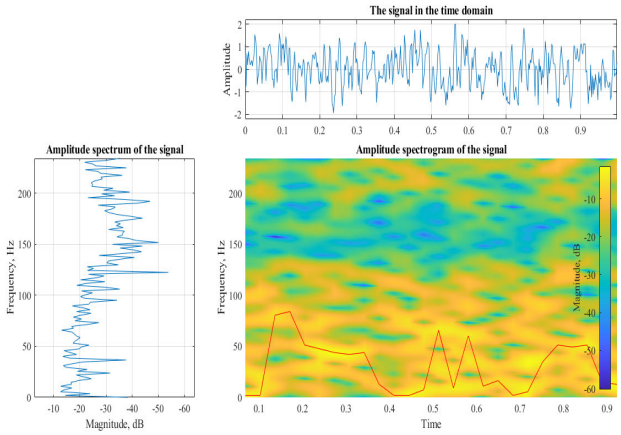

FIGURE 6. STFT result of the SPEI time series from January 1980 to December 2018.

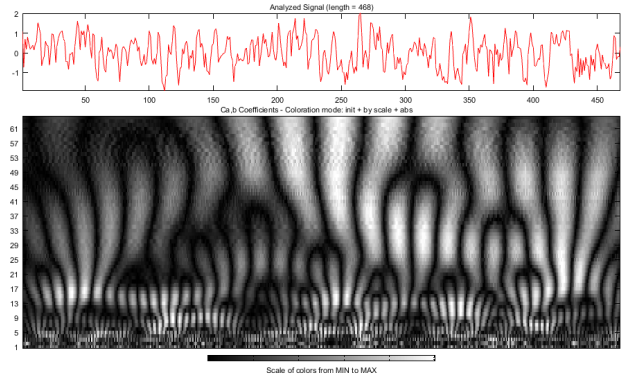

FIGURE 7. Monthly SPEI time series from January 1980 to December 2018 (upper), Real part of CWT (bottom) using Morlet 64 voices.

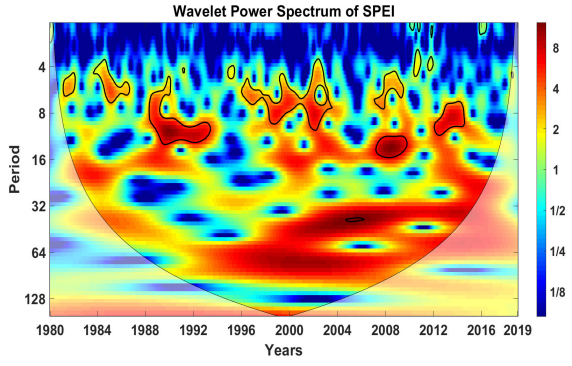

FIGURE 8. Wavelet power spectra analyses of SPEI time series from January 1980 to December 2018.

According to the figure 9a, the time series SPEI and VCI have a significant resonance period of 12-16 months from 2007 to 2011. The period is mainly in-phase during these years. Figure 9b displays that the time series SPEI and TCI have a period of 8-16 months for all years. From 2000 to 2006 years, and from 2006 to 2011 the periods are mainly in-phase; from 2011 to 2013, the periods are SPEI lagging TCI by 90-degree phase, and from 2013 to 2018, the periods are anti-phase. Figure 9c reveals that the time series SPEI and

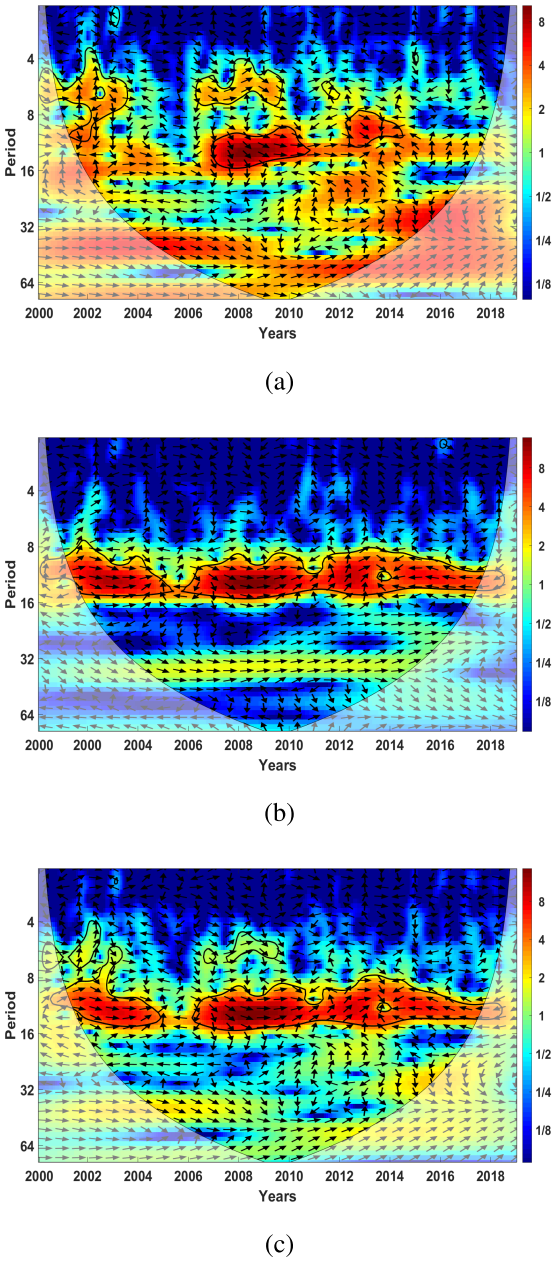

FIGURE 9. XWT: a) SPEI-VCI, b) SPEI-TCI and c) SPEI-VHI.

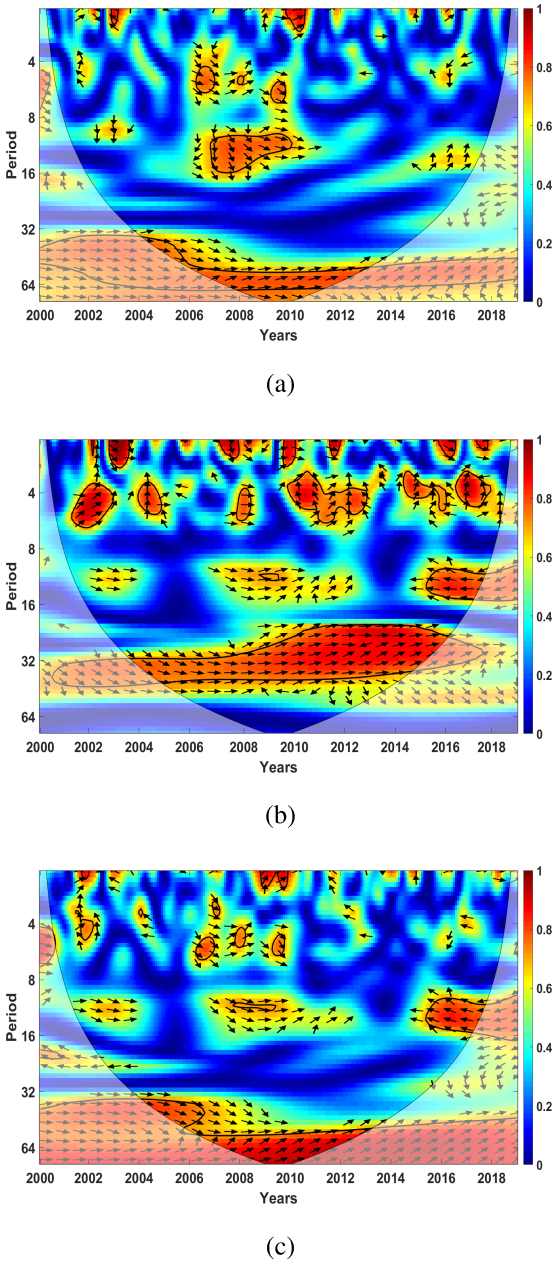

FIGURE 10. WTC: a) SPEI- VCI, b) SPEI-TCI and c) SPEI-VHI.

VHI have a period of 9-15 months from 2000 to 2005 and 2007 to 2018. From 2000 to 2005, and from 2007 to 2014 the periods are mainly in-phase, and from 2014 to 2018 the periods are anti-phase.

In order to estimate the coherence between satellite-based indices (VCI, TCI, and VHI) and meteorological index (SPEI) time series, WCT was applied and the results are illustrated in figure 10.

The results show that SPEI has significant coherence with VCI, TCI, and VHI in a 35-45 month period during all years. As an important outcome, a notable positive correlation was observed between the satellite-based indices and SPEI for the mentioned period. Besides, figure10a shows a coherence in 4-6-months and 10-16-month periods from 2007 to 2010. Figure 10b and figure 10c show that the SPEI is in anti-phase with TCI and VHI at 9-14-month period from 2016 to 2018. Also, a coherency was observed from 2007 to 2012 for the same period. The phase difference between SPEI and TCI from 2001 to 2002 and from 2015 to 2016 at the period of 3-7-months period is 30-45 degrees. In other words, SPEI lags behind TCI by 1-2 months.

V. CONCLUSION

In this study, the GEE platform was used to calculate satellite-based drought indices such as VCI, TCI, and VHI for the

Aegean Region. All results were displayed and the time series are also subtracted for frequency domain analysis.The SPEI was calculated as the meteorological station-based index. The frequency analysis of satellite-based indices finalized for the first time in the literature and the results were presented here. Moreover, the time-frequency analysis of SPEI was performed. The relationship between satellite-based and meteorological station-based time series was surveyed and presented using XWT and CWT tools. The study of time-frequency correlation and coherence between these time series (satellite-based and meteorological station-based) is also a novel inquiry.

ACKNOWLEDGMENT

The authors would like to thank the Turkish State Meteorological Service for providing the *In-situ* data free of charge.

REFERENCES

[1] D. A. Wilhite, "Drought as a natural hazard: Concepts and definitions," in *A Global Assessment*, vol. 1. London, U.K.: Routledge, 2000, ch. 1, pp. 3–18.

[2] R. Speed, D. Tickner, L. Gang, P. Sayers, W. Yu, L. Yuanyuan, C. Moncrieff, G. Pegram, L. Jianqiang, X. Xiangyu, L. Aihua, and Q. Bing, *Drought Risk Management: A Strategic Approach*. Paris, France: UNESCO Publishing, 2016.

[3] M. Svoboda, M. Hayes, and D. A. Wood, "Standardized precipitation index user guide," Meteorol. Org., Geneva, Switzerland, Tech. Rep., 2012, vol. 900.

[4] D. A. Wilhite, M. D. Svoboda, and M. J. Hayes, "Understanding the complex impacts of drought: A key to enhancing drought mitigation and preparedness," *Water Resour. Manage.*, vol. 21, no. 5, pp. 763–774, Apr. 2007. [Online]. Available: http://link.springer.com/10.1007/s11269-006-9076-5

[5] S. M. Vicente-Serrano, S. Beguería, J. Lorenzo-Lacruz, J. J. Camarero, J. I. López-Moreno, C. Azorin-Molina, J. Revuelto, E. Morán-Tejeda, and A. Sanchez-Lorenzo, "Performance of drought indices for ecological, agricultural, and hydrological applications," *Earth Interact.*, vol. 16, no. 10, pp. 1–27, Sep. 2012. [Online]. Available: https://journals.ametsoc.org/doi/10.1175/2012EI000434.1

[6] D. A. Wilhite and M. H. Glantz, "Understanding: The drought phenomenon: The role of definitions," *Water Int.*, vol. 10, no. 3, pp. 111–120, Jan. 1985. [Online]. Available: http://www.tandfonline.com/doi/abs/10.1080/02508068508686328

[7] A. K. Mishra and V. P. Singh, "A review of drought concepts," *J. Hydrol.*, vol. 391, nos. 1–2, pp. 202–216, Sep. 2010. [Online]. Available: https://linkinghub.elsevier.com/retrieve/pii/S0022169410004257

[8] A. Zargar, R. Sadiq, B. Naser, and F. I. Khan, "A review of drought indices," *Environ. Rev.*, vol. 19, pp. 333–349, Jul. 2011.

[9] Z. Hao and V. P. Singh, "Drought characterization from a multivariate perspective: A review," *J. Hydrol.*, vol. 527, pp. 668–678, Aug. 2015. [Online]. Available: https://linkinghub.elsevier.com/retrieve/pii/S0022169415003819

[10] A. AghaKouchak, A. Farahmand, F. S. Melton, J. Teixeira, M. C. Anderson, B. D. Wardlow, and C. R. Hain, "Remote sensing of drought: Progress, challenges and opportunities: Remote sensing of drought," *Rev. Geophys.*, vol. 53, no. 2, pp. 452–480, Jun. 2015. [Online]. Available: http://doi.wiley.com/10.1002/2014RG000456

[11] M. Svoboda and B. Fuchs, *Handbook of Drought Indicators and Indices* (Integrated Drought Management Tools and Guidelines Series). Geneva, Switzerland: World Meteorological Organization, 2016.

[12] T. B. McKee, N. J. Doesken, and J. Kleist, "The relationship of drought frequency and duration to time scales," in *Proc. 8th Conf. Appl. Climatol.*, Boston, MA, USA, 1993, vol. 17, no. 22, pp. 179–183.

[13] S. M. Vicente-Serrano, S. Beguería, and J. I. López-Moreno, "A multiscalar drought index sensitive to global warming: The standardized precipitation evapotranspiration index," *J. Climate*, vol. 23, no. 7, pp. 1696–1718, Apr. 2010. [Online]. Available: http://journals.ametsoc.org/doi/10.1175/2009JCLI2909.1

[14] S. Beguería, S. M. Vicente-Serrano, F. Reig, and B. Latorre, "Standardized precipitation evapotranspiration index (SPEI) revisited: Parameter fitting, evapotranspiration models, tools, datasets and drought monitoring," *Int. J. Climatol.*, vol. 34, no. 10, pp. 3001–3023, Aug. 2014. [Online]. Available: http://doi.wiley.com/10.1002/joc.3887

[15] L. Ji and A. J. Peters, "Assessing vegetation response to drought in the northern great plains using vegetation and drought indices," *Remote Sens. Environ.*, vol. 87, no. 1, pp. 85–98, Sep. 2003. [Online]. Available: https://linkinghub.elsevier.com/retrieve/pii/S0034425703001743

[16] C. J. Tucker and B. J. Choudhury, "Satellite remote sensing of drought conditions," *Remote Sens. Environ.*, vol. 23, no. 2, pp. 243–251, Nov. 1987. [Online]. Available: https://linkinghub.elsevier.com/retrieve/pii/003442578790040X

[17] I. Sandholt, K. Rasmussen, and J. Andersen, "A simple interpretation of the surface temperature/vegetation index space for assessment of surface moisture status," *Remote Sens. Environ.*, vol. 79, pp. 213–224, Feb. 2002. [Online]. Available: https://linkinghub.elsevier.com/retrieve/pii/S0034425701002747

[18] Y. Gu, E. Hunt, B. Wardlow, J. B. Basara, J. F. Brown, and J. P. Verdin, "Evaluation of MODIS NDVI and NDWI for vegetation drought monitoring using Oklahoma Mesonet soil moisture data," *Geophys. Res. Lett.*, vol. 35, no. 22, Nov. 2008, Art. no. L22401. [Online]. Available: http://doi.wiley.com/10.1029/2008GL035772

[19] A. Karnieli, N. Agam, R. T. Pinker, M. Anderson, M. L. Imhoff, G. G. Gutman, N. Panov, and A. Goldberg, "Use of NDVI and land surface temperature for drought assessment: Merits and limitations," *J. Climate*, vol. 23, no. 3, pp. 618–633, Feb. 2010. [Online]. Available: http://journals.ametsoc.org/doi/10.1175/2009JCLI2900.1

[20] N. T. Son, C. F. Chen, C. R. Chen, L. Y. Chang, and V. Q. Minh, "Monitoring agricultural drought in the lower Mekong basin using MODIS NDVI and land surface temperature data," *Int. J. Appl. Earth Observ. Geoinf.*, vol. 18, pp. 417–427, Aug. 2012. [Online]. Available: https://linkinghub.elsevier.com/retrieve/pii/S030324341200058X

[21] P.-X. Wang, X.-W. Li, J.-Y. Gong, and C. Song, "Vegetation temperature condition index and its application for drought monitoring," in *Proc. Scanning Present Resolving Future IEEE Int. Geosci. Remote Sens. Symp. (IGARSS)*, vol. 1, Jul. 2001, pp. 141–143.

[22] S. Shi, F. Yao, J. Zhang, and S. Yang, "Evaluation of temperature vegetation dryness index on drought monitoring over Eurasia," *IEEE Access*, vol. 8, pp. 30050–30059, 2020.

[23] F. N. Kogan, "Remote sensing of weather impacts on vegetation in non-homogeneous areas," *Int. J. Remote Sens.*, vol. 11, no. 8, pp. 1405–1419, Aug. 1990.

[24] A. L. Yagci, L. Di, and M. Deng, "The effect of corn–soybean rotation on the NDVI-based drought indicators: A case study in Iowa, USA, using vegetation condition index," *GISci. Remote Sens.*, vol. 52, no. 3, pp. 290–314, May 2015. [Online]. Available: http://www.tandfonline.com/doi/full/10.1080/15481603.2015.1038427

[25] F. N. Kogan, "Application of vegetation index and brightness temperature for drought detection," *Adv. Space Res.*, vol. 15, no. 11, pp. 91–100, Jan. 1995. [Online]. Available: https://linkinghub.elsevier.com/retrieve/pii/027311779500079T

[26] F. N. Kogan, "Global drought watch from space," *Bull. Amer. Meteorol. Soc.*, vol. 78, no. 4, pp. 621–636, Apr. 1997.

[27] F. N. Kogan, "Operational space technology for global vegetation assessment," *Bull. Amer. Meteorol. Soc.*, vol. 82, no. 9, pp. 1949–1964, 2001.

[28] N. Gorelick, M. Hancher, M. Dixon, S. Ilyushchenko, D. Thau, and R. Moore, "Google earth engine: Planetary-scale geospatial analysis for everyone," *Remote Sens. Environ.*, vol. 202, pp. 18–27, Dec. 2017. [Online]. Available: https://linkinghub.elsevier.com/retrieve/pii/S0034425717302900

[29] N. Sazib, I. Mladenova, and J. Bolten, "Leveraging the Google earth engine for drought assessment using global soil moisture data," *Remote Sens.*, vol. 10, no. 8, p. 1265, Aug. 2018. [Online]. Available: http://www.mdpi.com/2072-4292/10/8/1265

[30] I. N. Sneddon, *Fourier Transforms*. Chelmsford, MA, USA: Courier Corporation, 1995.

[31] R. N. Bracewell and R. N. Bracewell, *The Fourier Transform and its Applications*, vol. 31999. New York, NY, USA: McGraw-Hill, 1986.

[32] A. Dutt and V. Rokhlin, "Fast Fourier transforms for nonequispaced data," *SIAM J. Sci. Comput.*, vol. 14, no. 6, pp. 1368–1393, 1993.

[33] S. G. Mallat and Z. Zhang, "Matching pursuits with time-frequency dictionaries," *IEEE Trans. Signal Process.*, vol. 41, no. 12, pp. 3397–3415, Dec. 1993. [Online]. Available: http://ieeexplore.ieee.org/document/258082/

[34] S. Soltani, "On the use of the wavelet decomposition for time series prediction," *Neurocomputing*, vol. 48, nos. 1–4, pp. 267–277, Oct. 2002. [Online]. Available: https://linkinghub.elsevier.com/retrieve/pii/S0925231201006488

[35] A. B. Mabrouk, N. B. Abdallah, and Z. Dhifaoui, "Wavelet decomposition and autoregressive model for time series prediction," *Appl. Math. Comput.*, vol. 199, no. 1, pp. 334–340, May 2008.

[36] Y. Unal, T. Kindap, and M. Karaca, "Redefining the climate zones of Turkey using cluster analysis," *Int. J. Climatol.*, vol. 23, no. 9, pp. 1045–1055, Jul. 2003. [Online]. Available: http://doi.wiley.com/10.1002/joc.910

[37] B. Önol, "Effects of coastal topography on climate: High-resolution simulation with a regional climate model," *Climate Res.*, vol. 52, pp. 159–174, Mar. 2012. [Online]. Available: http://www.int-res.com/abstracts/cr/v52/p159-174/

[38] H. Kutiel and M. Türkeş, "Spatial and temporal variability of dryness characteristics in Turkey," *Int. J. Climatol.*, vol. 37, pp. 818–828, Aug. 2017.

[39] O. Hoegh-Guldberg, D. Jacob, M. Bindi, S. Brown, I. Camilloni, A. Diedhiou, R. Djalante, K. Ebi, F. Engelbrecht, J. Guiot, and Y. Hijioka, "Impacts of 1.5 °C global warming on natural and human systems," Global Warming 1.5 °C, IPCC Secretariat, IPCC Spec. Rep., 2018, pp. 175–311.

[40] C. Bhuiyan, R. P. Singh, and F. N. Kogan, "Monitoring drought dynamics in the Aravalli region (India) using different indices based on ground and remote sensing data," *Int. J. Appl. Earth Observ. Geoinf.*, vol. 8, no. 4, pp. 289–302, Dec. 2006.

[41] L. Du, Q. Tian, T. Yu, Q. Meng, T. Jancso, P. Udvardy, and Y. Huang, "A comprehensive drought monitoring method integrating MODIS and TRMM data," *Int. J. Appl. Earth Observ. Geoinf.*, vol. 23, pp. 245–253, Aug. 2013.

[42] V. A. Bento, C. M. Gouveia, C. C. DaCamara, and I. F. Trigo, "A climatological assessment of drought impact on vegetation health index," *Agricult. Forest Meteorol.*, vol. 259, pp. 286–295, Sep. 2018. [Online]. Available: https://www.sciencedirect.com/science/article/pii/S0168192318301667

[43] F. Kogan and W. Guo, "2006–2015 mega-drought in the western USA and its monitoring from space data," *Geomatics, Natural Hazards Risk*, vol. 6, no. 8, pp. 651–668, Nov. 2015. [Online]. Available: http://www.tandfonline.com/doi/full/10.1080/19475705.2015.1079265

[44] M. Abramowitz and I. A. Stegun, *Handbook of Mathematical Functions With Formulas, Graphs, and Mathematical Tables*, vol. 55. Washington, DC, USA: US Government Printing Office, 1964.

[45] C. W. Thornthwaite, "An approach toward a rational classification of climate," *Geograph. Rev.*, vol. 38, no. 1, p. 55, Jan. 1948. [Online]. Available: https://www.jstor.org/stable/210739?origin=crossref

[46] S. Rapuano and F. J. Harris, "An introduction to FFT and time domain windows," *IEEE Instrum. Meas. Mag.*, vol. 10, no. 6, pp. 32–44, Dec. 2007.

[47] F. J. Harris, "On the use of windows for harmonic analysis with the discrete Fourier transform," *Proc. IEEE*, vol. 66, no. 1, pp. 51–83, Jan. 1978.

[48] E. O. Brigham, *The Fast Fourier Transform and its Applications*. Upper Saddle River, NJ, USA: Prentice-Hall, 1988.

[49] M. Heideman, D. Johnson, and C. Burrus, "Gauss and the history of the fast Fourier transform," *IEEE ASSP Mag.*, vol. 1, no. 4, pp. 14–21, Oct. 1984. [Online]. Available: http://ieeexplore.ieee.org/document/1162257/

[50] A. I. Pasquini, K. L. Lecomte, E. L. Piovano, and P. J. Depetris, "Recent rainfall and runoff variability in central Argentina," *Quaternary Int.*, vol. 158, no. 1, pp. 127–139, Dec. 2006. [Online]. Available: https://linkinghub.elsevier.com/retrieve/pii/S1040618206001601

[51] J. C. Gutiérrez-Estrada and I. Pulido-Calvo, "Water temperature regimen analysis of intensive fishfarms associated with cooling effluents from power plants," *Biosyst. Eng.*, vol. 96, no. 4, pp. 581–591, Apr. 2007.

[52] İ. Dabanlı, A. K. Mishra, and Z. Şen, "Long-term spatio-temporal drought variability in Turkey," *J. Hydrol.*, vol. 552, pp. 779–792, Sep. 2017. [Online]. Available: https://linkinghub.elsevier.com/retrieve/pii/S0022169417305024

[53] D. Gabor, "Theory of communication," *J. Inst. Electr. Eng.*, vol. 93, no. 3, pp. 429–457, Nov. 1946.

[54] L. Cohen, "Time-frequency distributions—A review," *Proc. IEEE*, vol. 77, no. 7, pp. 941–981, Jul. 1989.

[55] T. Christopher and G. P. Compo, "A practical guide to wavelet analysis," *Bull. Amer. Meteorol. Soc.*, vol. 79, no. 1, pp. 61–78, 1998.

[56] K.-M. Lau and H. Weng, "Climate signal detection using wavelet transform: How to make a time series sing," *Bull. Amer. Meteorol. Soc.*, vol. 76, no. 12, pp. 2391–2402, Dec. 1995.

[57] M. Nakken, "Wavelet analysis of rainfall–runoff variability isolating climatic from anthropogenic patterns," *Environ. Model. Softw.*, vol. 14, no. 4, pp. 283–295, Jan. 1999.

[58] M. P. S. Echer, E. Echer, D. J. Nordemann, N. R. Rigozo, and A. Prestes, "Wavelet analysis of a centennial (1895–1994) southern Brazil rainfall series (Pelotas, 31°46′19″S 52°20′33″W)," *Climatic Change*, vol. 87, nos. 3–4, pp. 489–497, Apr. 2008.

[59] F. Soi-Kun, W. Chi-Sheng, W. Ting, H. Xia-Jiang, W. An-Yu, L. Ji, L. Bi-Qi, and L. Ka-Cheng, "Multiple time scale analysis of climate variation in Macau during the last 100 years," *J. Tropical Meteorol.*, vol. 18, no. 1, pp. 21–31, 2012.

[60] S. Beecham and R. K. Chowdhury, "Statistical behaviour of Adelaide's rainfall—Is climate change detectable?" in *Proc. World Environ. Water Resour. Congr.*, May 2008, pp. 1–13.

[61] C. K. Chui and J. Z. Wang, "An analysis of cardinal spline-wavelets," *J. Approximation Theory*, vol. 72, no. 1, pp. 54–68, Jan. 1993.

[62] B. Boashash, S. Touati, P. Flandrin, F. Hlawatsch, G. Tauböck, P. M. Oliveira, V. Barroso, R. Baraniuk, G. Jones, G. Matz, F. Hlawatsch, T. Alieva, M. J. Bastiaans, L. Galleani, A. O. Boudraa, F. Salzenstein, and A. Akan, "Advanced time-frequency signal and system analysis," in *Time-Frequency Signal Analysis and Processing: A Comprehensive Reference*. Amsterdam, The Netherlands: Elsevier, 2016, pp. 141–236.

[63] Y. Li, Y. Wen, H. Lai, and Q. Zhao, "Drought response analysis based on cross wavelet transform and mutual entropy," *Alexandria Eng. J.*, vol. 59, no. 3, pp. 1223–1231, Jun. 2020.

SEMRA KOCAASLAN received the B.S. degree in geomatics engineering and the M.S. degree in satellite communication and remote sensing from the Institute of Informatics, Istanbul Technical University (ITU), Turkey, in 2011 and 2013, respectively, where she is currently pursuing the Ph.D. degree in geographical information technologies (GIT) with the Department of Applied Informatics. Her research interests include natural disasters, remote sensing, and geographical information systems.

NEBİYE MUSAOĞLU received the B.S., M.S., and Ph.D. degrees from Istanbul Technical University, Istanbul, Turkey, in 1989, 1993, and 1999, respectively. From 1989 to 2000, she was a Research Assistant with the Department of Geomatics Engineering, Istanbul Technical University, where she was also an Associate Professor, from 2000 to 2006. She is currently a Full Professor with the Geomatics Engineering Department, Civil Engineering Faculty, Istanbul Technical University. She has authored or coauthored more than 150 articles. Her research interests include remote sensing and image processing.

SAEID KARAMZADEH received the M.S. and Ph.D. degrees from the Department of Communication Systems, Satellite Communication and Remote Sensing Program, Istanbul Technical University, in 2013 and 2015, respectively. He won the award for the most successful Ph.D. thesis with Istanbul Technical University. He is currently an Associate Professor with the Department of Electrical and Electronics Engineering, Bahçeşehir University. His research interests include microwave, antenna, remote sensing, and signal processing.